Biochemistry and Cell Biology
Biochimie et biologie cellulaire

Temporo-spacial micoranatomical distribution of the murine sodium-dependent ascorbic acid transporters Slc23a1 and Slc23a2 in the kidney throughout development

Journal:	*Biochemistry and Cell Biology*
Manuscript ID	bcb-2015-0090.R1
Manuscript Type:	Article
Date Submitted by the Author:	22-Nov-2016
Complete List of Authors:	Eck, Peter; University of Manitoba, Human Nutritional Sciences Corpe, Christopher; King's College London, Nutrition and Dietetics Levine, Mark; National Institutes of Health, Molecular and Clinical Nutrition Section
Keyword:	Slc23a1, Slc23a2, kidney, murine, development

Temporo-spacial micoranatomical distribution of the murine sodium-dependent ascorbic acid transporters *Slc23a1* and *Slc23a2* in the kidney throughout development

Peter K. Eck[§]*, Christopher Corpe*[$], Mark A. Levine*

[§]Corresponding Author:

Peter Eck
University of Manitoba, Department of Human Nutritional Sciences
W569 Duff Roblin Building, 190 Dysart Road
University of Manitoba, Winnipeg, MB R3T 2N2 Canada
Tel: 204 291 2917
e-mail: peter.eck@ad.umanitoba.ca

Author's institutional affiliations

[$]Corpe, Christopher
Department of Nutrition and Dietetics
Diabetes & Nutritional Sciences Division
School of Medicine
King's College London
Room 3.114 Franklin-Wilkins Building
150 Stamford Street
London SE1 9NH
Email: christopher.corpe@kcl.ac.uk

*Mark Levine, M.D.
Chief, Molecular and Clinical Nutrition Section
Senior Staff Physician
Building 10, Room 4D52 MSC 1372
National Institutes of Health
Bethesda, MD 20892-1372
Phone 301 402 5588
FAX 301 402 6436
Email MarkL@mail.nih.gov

Running Title: murine renal *Slc23a1* and *Slc23a1*

Key words: *Slc23a1*, *Slc23a2*, kidney, murine, development

Abstract

The two membrane transporters Slc23a1 and Slc23a2 mediate ascorbic acid uptake into cells. We recently determined the key role of Slc23a1 in renal re-absorption of ascorbic acid in a knockout mouse model. However, the renal spatial and temporal expression patterns of murine *Slc23a1* and *Slc23a2* are not defined. This study utilizes database evidence combined with experimental confirmation via *in situ hybridization* to define spatial and temporal expression of *Slc23a1* in the murine kidney. *Slc23a1* is expressed in the early proximal tubule, but not in its precursors during embryonic development, and exclusive proximal tubular expression persists throughout the animal's lifetime. In contrast, *Slc23a2* is uniformly expressed in metabolic cell types such as stromal cells. The expression patterns appear to be conserved from rodent lineages to humans.

Introduction

Ascorbic acid (ascorbate, Vitamin C) is an indispensable metabolite essential for survival. Ascorbate cannot be synthesized in humans due to a loss of functional gulonolactone oxidase (EC 1.1.3.8), but is synthesized in murine species, such as mouse and rat (Padayatty et al. 2003; Nishikimi et al. 1988). The kidney is a central organ for ascorbic acid homeostasis. Slc23a1 plays a key role in ascorbate homeostasis and pharmacokinetics, as demonstrated by the facts that *Slc23a1*$^{-/-}$ knockout mice have very high urinary losses leading to low systemic concentrations (Corpe et al. 2010). Slc23a1 is known to mediate ascorbic acid uptake into epithelial cells of the small intestine, liver and kidney (Boyer et al. 2005; Lee et al. 2006; Luo et al. 2008; Maulen et al. 2003; Varma et al. 2008), and is also expressed in some epithelia of the reproductive system and the brain (Tsukaguchi et al. 1999). Slc23a1 transports ascorbic acid with comparatively low affinity (K_m≈250 μM) but high capacity, reflecting its role in intestinal absorption and renal re-absorption (Daruwala et al. 1999; Tsukaguchi et al. 1999). Compared to wildtype controls, the *Slc23a1*$^{-/-}$ mouse has up to an 18-fold increase in fractional ascorbate excretion. The consequence is that ascorbate renal reabsorption is lost, resulting in low plasma and tissue concentrations and high perinatal loss of offspring (Corpe et al. 2010).

A second ascorbic acid transporter, *Slc23a2*, is found in almost all cell types, mediates ascorbic acid transport across cell membranes with high affinity (K_m 15 μM), and requires cations (Na^+, Ca^{2+}, or Mg^{2+}) for optimal activity (Daruwala et al. 1999; Godoy et al. 2007; Tsukaguchi et al. 1999). The global elimination of *Slc23a2* results in undetectable ascorbate tissue concentrations, and *Slc23a2*$^{-/-}$ mice died within minutes of birth (Sotiriou et al. 2002). Due to its expression in a wide range of tissues it is generally accepted that Slc23a2 is responsible for ascorbate tissue accumulation needed for survival (Sotiriou et al. 2002).

Despite the importance of both sodium-dependent ascorbic acid transporters and the fact that both genes have been eliminated in mouse models, their spatial expression in defined anatomical compartments of the nephron and the temporal expression during embryonic development are not described for murine species. This study reports the temporal-spatial distribution of the murine *Slc23a1* and *Slc23a2* transcripts throughout kidney developmental stages by comparing *in situ hybridization* (ISH), microarray and quantitative PCR data of nephron compartments.

Materials and Methods

In Situ Hybridizations

Organ samples: Samples were obtained from embryonic mice and adult rats as part of animal protocols approved by the Eunice Kennedy Shriver National Institute of Child Health and Human Development and the National Institute of Diabetes and Digestive and Kidney Diseases Animal Care and Use Committees. Specimens were harvested, snap frozen in dry ice and stored at -70°C. Serial sections of 10 µm thickness were cut at -15°C and thaw-mounted onto poly-L-lysine-coated slides for in situ hybridization or immunohistochemistry.

Probes Hybridization and Visualization: The human *SLC23A1* and *SLC23A2* complete coding sequences subcloned into pGEM®-T Easy Vectors (Promega) were used to prepare RNA probes for in situ hybridizations (Daruwala et al. 1999). The synthesis of ^{35}S-labeled cRNA probes, and the hybridization and visualization procedures have been previously described in detail (Bondy et al. 1993).

Renal gene expression analysis in adult rats

Microdissection: Male Sprague-Dawley rats (250-300g) were anesthetized by an intraperitoneal injection of 120 mg/kg thiobarbitural. After interruption of the aortic blood flow to the kidney it was perfused with 30 ml cold PBS (Sigma Chemical, St Louis, MO) followed by 30 ml culture medium [Dubelcco`s modified Eagle`s Medium (DMEM), Sigma Chemical, St Louis, MO] containing 1 mg/ml collagenase (*Clostridium histolyticum*, Sigma Chemical). The kidney was then removed, cut into slices, and incubated in the DMEM/collagenase solution for 22 minutes at 37°C. Microdissection was performed with sharpened forceps at 4°C under a stereomicroscope. The lengths of dissected segments were determined with an eyepiece micrometer. In general, 6 to 10 mm of tubule segments were dissected and pooled to constitute one sample. The following specimens were dissected: glomeruli (Glm), proximal straight tubules (PST), proximal convoluted tubules (PCT),

medullary thick ascending limb (mTAL), cortical thick ascending limb (cTAL), macula densa containing segment (MDCS), cortical collecting duct (CCD), outer medullary collecting duct (OMCD), inner medullary collecting duct (IMCD). Segments of the proximal convoluted tubule (PCT) may have contained S1 and S2 segments, but not S3 segments. Samples were placed in 100 µl guanidine isothiocyanate buffer (GITC buffer: 4 M guanidine isothiocyanate, 25 mM sodium acetate, 0.8% β-mercatoethanol, pH 6.0), snap frozen in liquid nitrogen and stored at –80°C.

RNA isolation: RNA from the renal samples were thawed in ice slurry and sonicated for 15 seconds. Twenty micrograms of E-coli ribosomal RNA (Boehringer, Mineapolis) was added as carrier. The 100ul sample in GITC buffer was layered onto a gradient of cesium chloride (100 µl of 97%, 20 µl of 40% cesium chloride in 25 mM sodium acetate buffer) in a 250 µl polycarbonate ultracentrifuge tube. Samples were centrifuged for two hours at 100000 g in a Beckman TLA 100 ultracentrifuge (Beckman Instruments, Fullerton) with a fixed angled rotor. The resulting RNA pellet was dissolved in 0.3 M sodium acetate and precipitated with ethanol. The purified RNA was dissolved in diethyl pyrocarbonate treated water containing 20 U RNAsin.

Reverse transcription: Reverse transcription was performed in the presence of 100IU Moloney murine leukemia virus reverse transcriptase (Superscript BRL, Gaithersburg), 0.5 µg oligo$(dT)_{12\text{-}18}$ (Pharmacia, Piscataway), 20 IU RNAsin (Promega, Madison), 10 mM dithiothreitol, 0.5 mM dNTP (Pharmacia), and 1% bovine serum albumin (Boehringer) in the buffer provided by the manufacturer in 20 µl. Prior to the addition of reverse transcriptase the reaction mixture was heated to 65°C for 5 minutes to allow annealing of the primers. cDNA was synthesized at 42°C for one hour and precipitated with 1 µl of linear acrylamide, 4 M ammonium acetate in 100% ethanol. The pellet was redissolved in Tris-EDTA buffer adjusted so that each 2 µl of cDNA corresponded to 1 mm of segment dissected.

Polymerase chain reaction: In each experiment, all tubes were assayed for expression of *Slc23a1* and *Slc23a2*. Rat specific primer were designed and optimized from the known sequences NM017315 and NM017315, respectively. The following primer pair was chosen and optimized to amplify a 719 bp piece in between base 1021 and base 1740 of the published r-Slc23a1 cDNA open reading frame sequence. Sense: 5`-TCATCGAGTCCATCGGTG-3`, antisense: 5`-AGAATCCTCTGAAGACTG-3`. A 779 bp fragment of r-Slc23a2 was amplified with the sense primer 5`-GACGTCTTCCCTTCCAAC-3` and the antisense primer 5`-CTTGTTTCCTTTGCTCAC-3` between base 1201 and 1980 of the published r-Slc23a2 open reading frame sequence. The primers for both amplifications are located near or in part in the 3` end of the coding region to ensure optimum detection of the cDNA. Amplification conditions included the following: 0.5 µM of each primer, 50 mM KCL, 10 mM Tris- HCl, 2,5 mM MgCl, 200 µM of dATP, dCTP and dTTP, 50 µM dGTP and 150 µM 7-deaza-2'GTP, as well as Taq DNA polymerase (Life Technologies). The amplification conditions were as follow: 5 min denaturation at 94 C followed by 35 cycles of 94 for 30 s, 55 for 30 s and 72 for 30 s. A final extension at 72 for 5 min was performed. Amplification products were confirmed by gel electrophoresis and compared to known DNA standards for estimation of the fragment size. The relative intensity of each PCR product band on the ethidium bromide gel was assessed by optical density. The identities of the PCR products were confirmed by sequencing using the dideoxynucleotide chain termination method on an automatic sequencer (ABI PRISM 377, Perkin Elmer, Foster City, CA) using the manufacturer's supplies. Sequence data were analyzed using Sequencher 4.1 (Genes Codes Corporation, Ann Arbor, MI).

Renal gene expression analysis in the developing mouse

We re-analyzed the entire kidney development dataset generated with Affymetrix MOE430 version 2 microarray, which is available for the GenitoUrinary Development Molecular

157 Anatomy Project (GUDMAP.org) (Harding et al. 2011; McMahon et al. 2008). Gene
158 expression data from 54 microarrays were analyzed for the expression of *Slc23a1* after
159 downloading the individual excel files for different nephron segments at different
160 developmental stages. Data were transformed into relative fluorescent units and graphically
161 displayed. The protocols for the generation of the tissue samples can be found at the
162 GUDMAP protocol web site: http://www.gudmap.org/Research/Protocols. Expression data
163 for the medullary collecting duct, cortical collecting duct and collecting duct distal to the last
164 branch point, S-shaped body, urothelium of the ureter, medullary interstitium, forming
165 muscle layer surrounding the urothelium (ureteral mesenchyme), loop of Henle (including
166 cortical anlage of the loop of Henle and medullary immature loop of Henle), and the proximal
167 tubule were obtained and processed.
168 Corresponding ISH images were obtained from the GUDMAP web server, the protocols used
169 for tissue isolation, sectioning, in situ hybridization and imaging are available at the protocols
170 web site: http://www.gudmap.org/Research/Protocols.
171

Results

Murine *Slc23a1* is exclusively expressed in the renal proximal tubule

Earliest embryonic *Slc23a1* expression can be detected 14 days post conception in the developing kidney (Figure 1A) and emerging gene expression is confirmed in the developing early proximal tubule at embryonic day E15.5 (Figures 1B, 1D). *Slc23a1* is not expressed in the precursors of the early proximal tubule, such as the capping mesenchymal, renal vesicle, and S-shaped body (Figure 1D). The nephron is derived from capping mesenchymal cells, which undergo a mesenchymal-to-epithelial transition to form the renal vesicle. The cells of the renal vesicle differentiate, elongate, and convolute to form an S-shaped body, from which the glomerulus, proximal tube, loop of Henle and distal tubule are derived.

In the late stage embryo, at day 18 post conception, the *Slc23a1* transcript is strongly expressed in the maturing renal cortex, and outside the kidney significant expression can be confirmed in the small intestinal loops and the liver (Figure 1C). The proximal tubule is the only renal anatomic compartment where *Slc23a1* is expressed in significant amounts in late embryos, starting at day 14 (Figure 1A) and clearly distinguishable from all other parts of the nephron at day 15.5 (Figure 2A). This expression pattern remains stable in the juvenile and adult kidney (Figures 2B, 2C, 2D). *In situ* hybridizations of the adult murine kidney shows the *Slc23a1* message in a ray-like pattern beginning at the border of the outer medulla and extending into the renal cortex (Figure 2D), consistent with a typical proximal tubule anatomic distribution (Chin et al. 1997). This spatial distribution is confirmed by the more sensitive and detailed dark field micrography (Figures 3A, 3B), and RT-PCR on micro-dissected nephron compartments (Figures 3C), mapping *Slc23a1* mRNA expression to the proximal convoluted and straight tubules of the adult murine kidney.

195 Murine *Slc23a2* is uniformly expressed throughout the murine kidney

196 *Slc23a2* mRNA is uniformly expressed throughout the murine late stage embryonic body
197 without signs of defined organ specific patterns (Figures 4A, 4B) and it does not show a
198 distinct distribution in the adult kidney (Figure 4C, 4D, 4E). In renal microdissected segments
199 *Slc23a2* is found in moderate levels, in a relative uniform distribution (Figure 4F), except that
200 levels are close to the detection limit in the proximal convoluted and straight tubule. This
201 likely indicates a lack of expression in the proximal convoluted and straight tubules, where
202 *Slc23a1* is expressed. Highest *Slc23a2* expression is located in the inner medullary collecting
203 duct, indicating expression by stromal fibroblasts (Chin et al. 1997).

204

Discussion

In this report we resolve the temporal and spatial expression of the *Slc23a1* and *Slc23a2* transcripts in the developing and mature murine kidney. The presented data derived from ISH, microarray and RT-PCR analysis consistently demonstrate that *Slc23a1* expression is exclusively limited to the proximal tubule during renal development and in the adult kidney. Thus, *Slc23a1* is one of the rare genes displaying extreme component specific expression (Brunskill et al. 2009). Remarkably, the overwhelming majority of genes with a similar expression pattern encode either known membrane transporters or membrane associated proteins of unknown functions (Brunskill et al. 2009), demonstrating the essential function of the proximal tubule in re-absorption of vitamins and organic compounds/metabolites.

These data of exclusive *Slc23a1* expression in the murine renal proximal convoluted and straight tubules are consistent with the expression pattern reported for the human transcript (Corpe et al. 2010; Eck et al. 2013). This is also consistent with the assumption that gene expression throughout renal development is highly conserved between mammalian species (Thiagarajan et al. 2011). Twenty-five distinct renal cell types are known, which are derived from two intermediate mesoderm-derived cell populations: the metanephric mesenchyme and the ureteric bud. The ureteric bud forms a dichotomously branching epithelial tree, giving rise to the cell types that make up the collecting ducts of the kidney and the ureter that connects the kidney with the bladder (Thiagarajan et al. 2011). Before its appearance in the early proximal tubule, *Slc23a1* is not expressed in any precursor tissues, such as the capping mesenchyme surrounding the ureteric bud, which gives rise to the renal vesicle. The renal vesicle then elongates and convolutes to form the S-shaped body, which subsequently gives rise to the glomerulus, proximal tubule, loop of Henle, and distal tubule (Brunskill et al. 2009). *Slc23a1* is not expressed in the ureteric bud derivatives, forming the

tip and non-tip sections in the cortex, and the medullary region, to shape the collecting duct system. Expression is also absent in the cortical and medullary interstitium or stroma.

The key role of the ascorbic acid uptake protein Slc23a1 in the maintenance of systemic vitamin C levels was revealed through *Slc23a1*$^{-/-}$ mice (Corpe et al. 2010). For example, female *Slc23a1*$^{-/-}$ mice had an 18 fold increase in fractional excretion of ascorbate in the kidney, and a 70% decrease in circulating vitamin C concentrations compared to wildtypes. This strongly indicated that Slc23a1 is the only ascorbic acid uptake protein on the apical side of the renal proximal epithelial cell (Corpe et al. 2010; Eck et al. 2013). However, these functional data on the *Slc23a1*$^{-/-}$ mouse did not rule out the possible disruption of proper kidney development as a contributing factor to renal ascorbic acid losses. The temporal and spatial expression patterns described above clearly identify *Slc23a1's* sole function in the cellular transport of ascorbic acid, ruling out a function in development, cell adhesion and cell-cell communication (Brunskill et al. 2009). We therefore rule out a role as an "anlage in statu nascendi" gene, which would be important in the formation of a structure by showing earlier expression in the anlage (Brunskill et al. 2009). The earliest *Slc23a1* expression is detectable in stage IV nephrons, which is the maturing nephron (Thiagarajan et al. 2011), and persists through adulthood. This also confirms that segmentation of the early nephron into proximal, distal and Loop of Henle elements does not occur until the formation of a stage IV nephron (Thiagarajan et al. 2011). These expression patterns in adult murine are identical to the human site of expression (Eck et al. 2013), allowing an extrapolation to the basic biology of the transporter in humans.

In contrast to the much defined temporal-spatial *Slc23a1* expression in the murine kidney, *Slc23a2* is found in moderate levels and relative uniform distribution pattern, consistent with expression by stromal fibroblasts (Chin et al. 1997). *Slc23a2* is undetectable in the proximal convoluted and straight tubule, ruling out any role in renal ascorbic acid

reabsorption, and confirming the notion that Slc23a2 is responsible for ascorbic acid distribution into metabolically active stromal cells (Sotiriou et al. 2002).

ACKNOWLEDGEMENT

Mark Levine's contributions were funded through the National Institute of Diabetes and Digestive and Kidney Diseases intramural program grant numbers Z1A DK053218 06 and Z1A DK054506 15. Peter Eck was supported by a NSERC Canada Research Chair in Nutrigenomics.

Carolyn A. Bondy and Jie Wang (NHLBI) contributed some in situ hybridization images.

Jurgen Schnerman (NIDDK) provided the micro-dissected nephron samples.

This study used data from the GUDMAP database http://www.gudmap.org [microarray and ISH images downloaded in January 2015]. ISH selected from dataset GUDMAP:9176, principal investigator Melissa H Little, University of Queensland, Brisbane, Australia.

DISCLOSURE

The authors have no competing interest to disclose.

References

Bondy C, Zhou J, Lee W 1993. In situ hybridization histochemistry. In: Pablo F, Scanes C (eds) Handbook of Endocrine Research Techniques. 13 edn. Academic Press, New York, pp 266–288

Boyer JC, Campbell CE, Sigurdson WJ, Kuo SM 2005. Polarized localization of vitamin C transporters, SVCT1 and SVCT2, in epithelial cells. Biochem Bioph Res Co 334 (1):150-156.

Brunskill EW, Aronow BJ, Georgas K, Rumballe B, Valerius MT, Aronow J, Kaimal V, Jegga AG, Yu J, Grimmond S, McMahon AP, Patterson LT, Little MH, Potter SS 2009. Atlas of Gene Expression in the Developing Kidney at Microanatomic Resolution (vol 15, pg 781, 2008). Developmental Cell 16 (3):482-482.

Chin E, Zamah AM, Landau D, Gronboek H, Flyvbjerg A, Leroith D, Bondy CA 1997. Changes in facilitative glucose transporter messenger ribonucleic acid levels in the diabetic rat kidney. Endocrinology 138 (3):1267-1275

Corpe CP, Tu H, Eck P, Wang J, Faulhaber-Walter R, Schnermann J, Margolis S, Padayatty S, Sun H, Wang Y, Nussbaum RL, Espey MG, Levine M 2010. Vitamin C transporter Slc23a1 links renal reabsorption, vitamin C tissue accumulation, and perinatal survival in mice. Journal of Clinical Investigation 120 (4):1069-1083

Daruwala R, Song J, Koh WS, Rumsey SC, Levine M 1999. Cloning and functional characterization of the human sodium-dependent vitamin C transporters hSVCT1 and hSVCT2. FEBS Lett 460 (3):480-484

Eck P, Kwon O, Chen S, Mian O, Levine M 2013. The human sodium-dependent ascorbic acid transporters SLC23A1 and SLC23A2 do not mediate ascorbic acid release in the proximal renal epithelial cell. Physiological Reports 1 (6):e00136.

297 Godoy A, Ormazabal V, Moraga-Cid G, Zúñiga FA, Sotomayor P, Barra V, Vasquez O,
298 Montecinos V, Mardones L, Guzmán C, Villagrán M, Aguayo LG, Oñate SA, Reyes
299 AM, Cárcamo JG, Rivas CI, Vera JC 2007. Mechanistic insights and functional
300 determinants of the transport cycle of the ascorbic acid transporter SVCT2: Activation
301 by sodium and absolute dependence on bivalent cations. Journal of Biological
302 Chemistry 282 (1):615-624
303 Harding SD, Armit C, Armstrong J, Brennan J, Cheng Y, Haggarty B, Houghton D, Lloyd-
304 MacGilp S, Pi X, Roochun Y, Sharghi M, Tindal C, McMahon AP, Gottesman B,
305 Little MH, Georgas K, Aronow BJ, Steven Potter S, Brunskill EW, Michelle
306 Southard-Smith E, Mendelsohn C, Baldock RA, Davies JA, Davidson D 2011. The
307 GUDMAP database - an online resource for genitourinary research. Development 138
308 (13):2845-2853
309 Lee JH, Oh CS, Mun GH, Kim JH, Chung YH, Hwang YI, Shin DH, Lee WJ 2006.
310 Immunohistochemical localization of sodium-dependent L-ascorbic acid transporter 1
311 protein in rat kidney. Histochemistry and Cell Biology 126 (4):491-494.
312 Luo S, Wang Z, Kansara V, Pal D, Mitra AK 2008. Activity of a sodium-dependent vitamin
313 C transporter (SVCT) in MDCK-MDR1 cells and mechanism of ascorbate uptake. Int
314 J Pharm
315 Maulen NP, Henriquez EA, Kempe S, Carcamo JG, Schmid-Kotsas A, Bachem M, Grunert
316 A, Bustamante ME, Nualart F, Vera JC 2003. Up-regulation and polarized expression
317 of the sodium-ascorbic acid transporter SVCT1 in post-confluent differentiated CaCo-
318 2 cells. J Biol Chem 278 (11):9035-9041
319 McMahon AP, Aronow BJ, Davidson DR, Davies JA, Gaido KW, Grimmond S, Lessard JL,
320 Little MH, Potter SS, Wilder EL, Zhang P 2008. GUDMAP: The genitourinary
321 developmental molecular anatomy project. J Am Soc Nephrol 19 (4):667-671

322 Nishikimi M, Koshizaka T, Ozawa T, Yagi K (1988) Occurrence in humans and guinea pigs
323 of the gene related to their missing enzyme L-gulono-γ-lactone oxidase. Arch
324 Biochem Biophys 267 (2):842-846
325 Padayatty SJ, Katz A, Wang Y, Eck P, Kwon O, Lee JH, Chen S, Corpe C, Dutta A, Dutta
326 SK, Levine M 2003. Vitamin C as an antioxidant: Evaluation of its role in disease
327 prevention. Journal of the American College of Nutrition 22 (1):18-35
328 Sotiriou S, Gispert S, Cheng J, Wang YH, Chen A, Hoogstraten-Miller S, Miller GF, Kwon
329 O, Levine M, Guttentag SH, Nussbaum RL 2002. Ascorbic-acid transporter Slc23a1
330 is essential for vitamin C transport into the brain and for perinatal survival. Nature
331 Medicine 8 (5):514-517.
332 Thiagarajan RD, Georgas KM, Rumballe BA, Lesieur E, Chiu HS, Taylor D, Tang DTP,
333 Grimmond SM, Little MH 2011. Identification of Anchor Genes during Kidney
334 Development Defines Ontological Relationships, Molecular Subcompartments and
335 Regulatory Pathways. PLoS One 6 (2).
336 Tsukaguchi H, Tokui T, Mackenzie B, Berger UV, Chen XZ, Wang Y, Brubaker RF, Hediger
337 MA 1999. A family of mammalian Na+-dependent L-ascorbic acid transporters.
338 Nature 399 (6731):70-75
339 Varma S, Campbell CE, Kuo SM 2008. Functional role of conserved transmembrane segment
340 1 residues in human sodium-dependent vitamin C transporters. Biochemistry 47
341 (9):2952-2960
342

Figure Captions

Figure 1: *Slc23a1* expression in morphological structures of the developing murine and its kidney assed through *in situ* hybridisation (dark areas indicate expression) and microarray analysis. (**A**) *Slc23a1* expression in the mouse embryo 14.5 days post conception (E14.5) emerging in the kidney (Ki). (**B**) *Slc23a1* expression in kidney of the mouse embryo at 15.5 days post conception (E15.5). (**C**) *Slc23a1* expression in the mouse embryo 18 days post conception (E18) showing well-defined ray-like pattern in the maturing renal cortex (Ki), as well as defined patterns in small intestinal loops (Si) and the liver (Li). (**D**) Sense *Slc23a1* cRNA hybridized to a slide corresponding with figure 1C. (**E**) Temporal *Slc23a1* expression in developmental precursors of the proximal tubule assessed by microarray analysis and expressed as relative fluorescent units (RFU).

Figure 2: *Slc23a1* expression in micro-anatomical compartments of the late embryonic, postpartum and adult murine kidney assed through microarray analysis and *in situ* hybridisation (dark areas indicate expression). (**A**) *Slc23a1* expression in segments of the embryonal murine nephron at day 15.5 post conception (E15.5) expressed as Relative Fluorescent Units (RFU) from microarrays. (**B, C**) *Slc23a1* expression in the kidney of a seven day old mouse. (**D**) *Slc23a1* expression in the adult murine kidney at the border of the outer medulla (OM).

Figure 3: *Slc23a1* expression in micro-anatomical compartments of the adult murine kidney. **(A)** *Slc23a1* expression in the adult murine kidney using a dark field micrograph shows expression in proximal tubules (PT, light spots), but no signal in vascular bundles (VB, dark areas) or the ascending thick limbs of Henle localized in the medullary rays (MR, dark areas). **(B)** Haematoxylin and eosin stained (H&E) bright field image corresponding to image 3A. Here, PT, VB and MR were microscopically identified by a pathologist. (**C**) *Slc23a1*

expression in dissected nephron segments from the adult murine kidney assessed with quantitative PCR expressed as Relative Band Fluorescent Units (RBFU).

Figure 4: *Slc23a2* expression in the murine kidney assessed by ISH (A, B, C), dark field micrographs (D, E), and quantitative PCR (F). (**A**) *Slc23a2* expression in the mouse embryo at day 18 (E18). (**B**) Corresponding image to figure 4A hybridized with sense RNA. (**C**) *Slc23a2* expression in the adult murine kidney. (**D**) *Slc23a2* expression in the adult murine kidney using a dark field micrograph shows relatively uniform expression. **(E)** Haematoxylin and eosin stained (H&E) bright field image corresponding to image 4D. Here, PT, VB and MR were microscopically identified by a pathologist. (**F**) *Slc23a2* expression in dissected nephron segments from the adult murine kidney assessed with quantitative PCR expressed as Relative Band Fluorescent Units (RBFU).

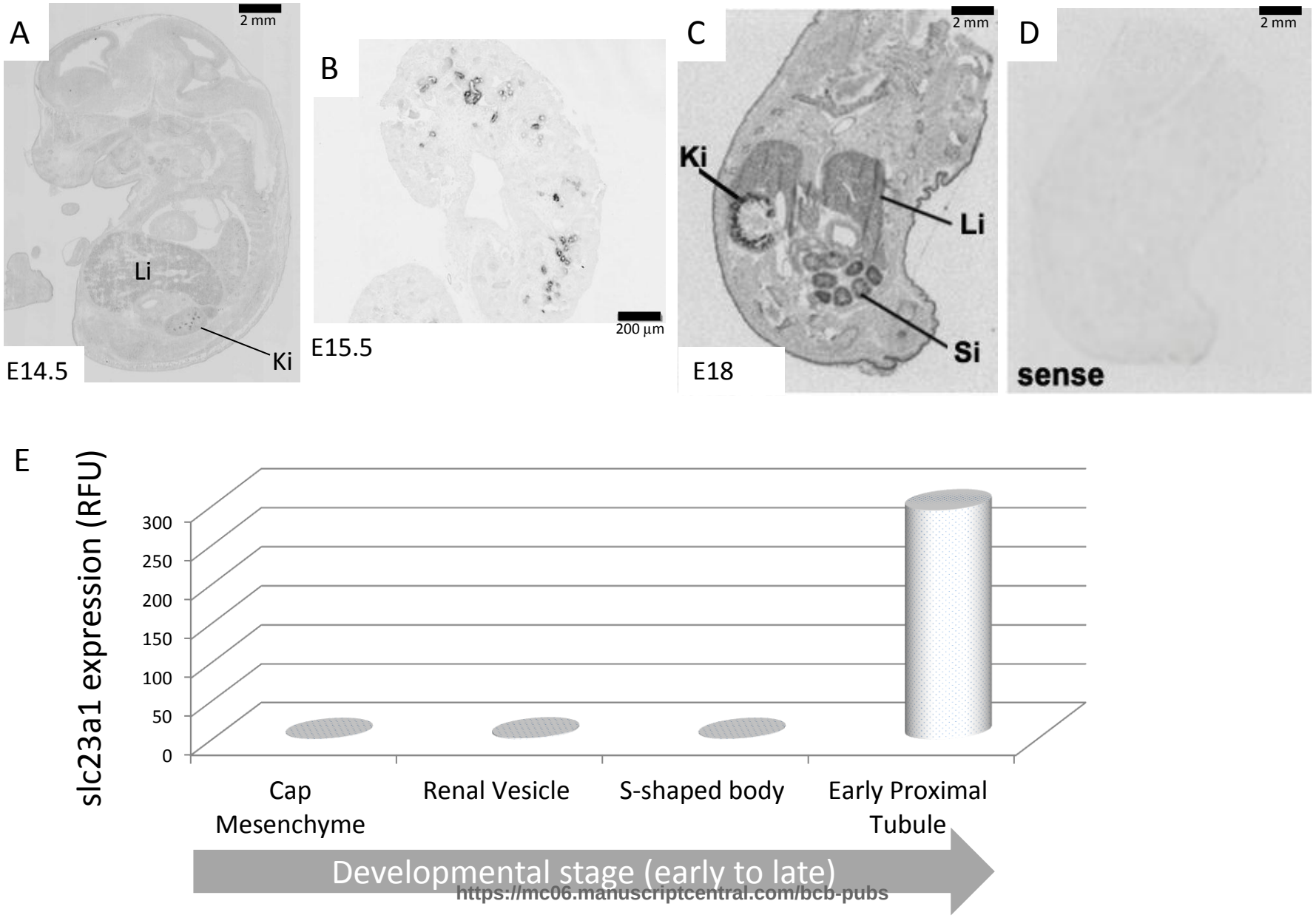
A
2 mm
Li
Ki
E14.5
B
200 µm
E15.5
C
2 mm
Ki
Li
Si
E18
D
2 mm
sense
E
slc23a1 expression (RFU)
300
250
200
150
100
50
0
Cap Mesenchyme
Renal Vesicle
S-shaped body
Early Proximal Tubule
Developmental stage (early to late)

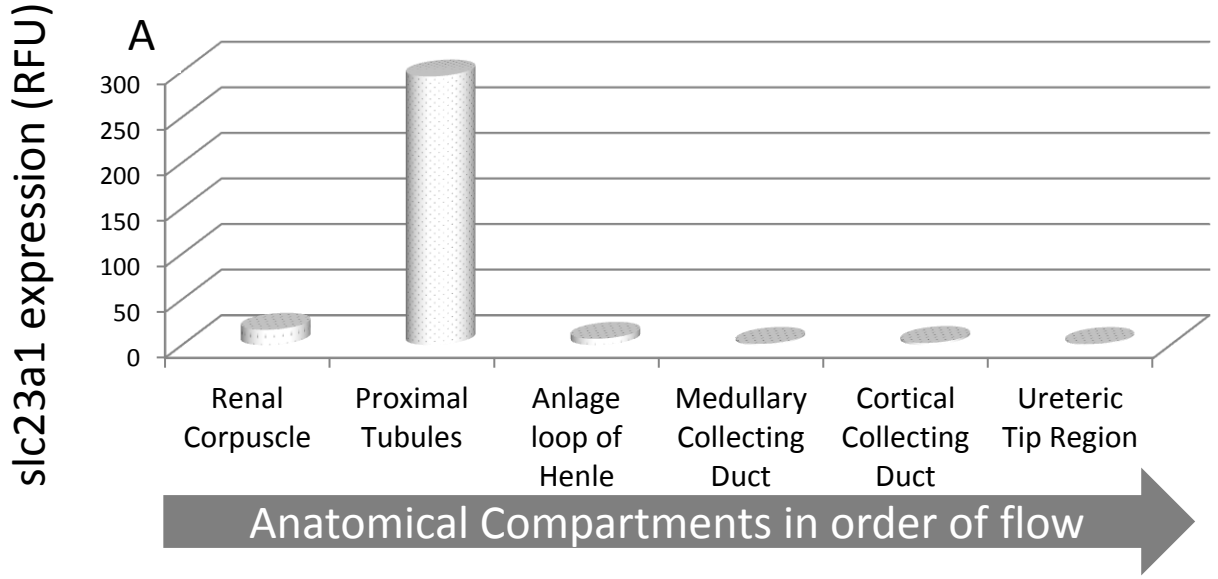
A
slc23a1 expression (RFU)
300
250
200
150
100
50
0
Renal Corpuscle
Proximal Tubules
Anlage loop of Henle
Medullary Collecting Duct
Cortical Collecting Duct
Ureteric Tip Region
Anatomical Compartments in order of flow

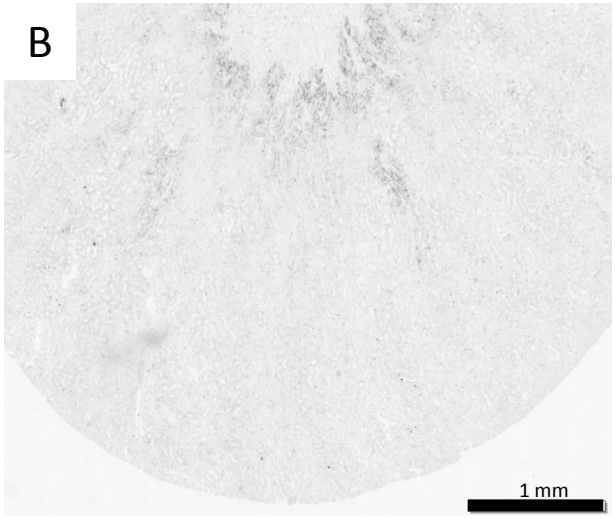
B
1 mm

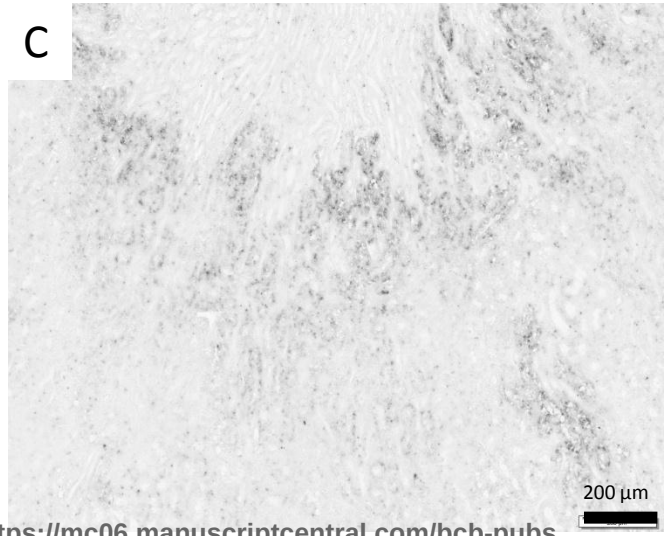
C
200 µm

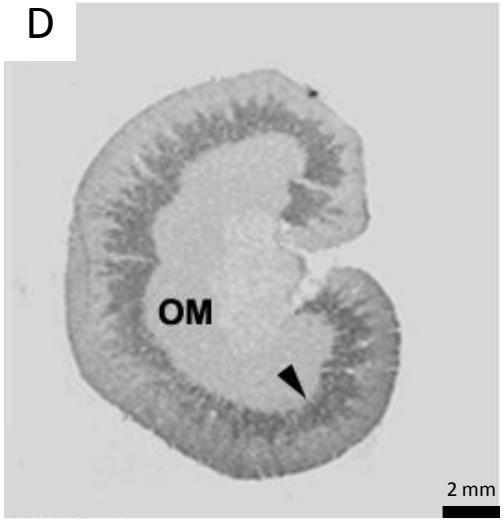
D
OM
2 mm

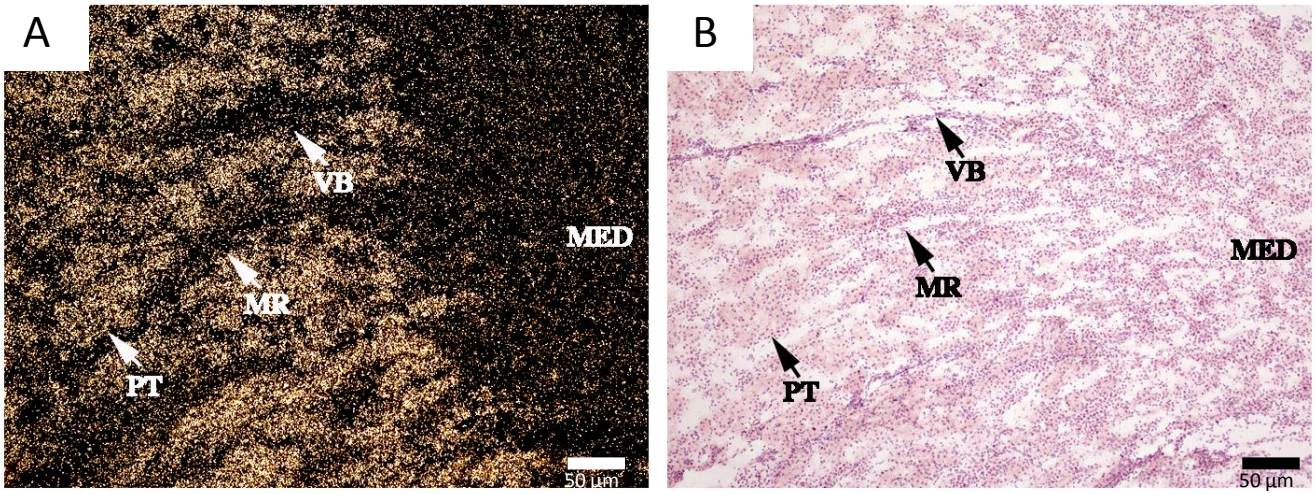
A
VB
MED
MR
PT
50 µm
B
VB
MED
MR
PT
50 µm

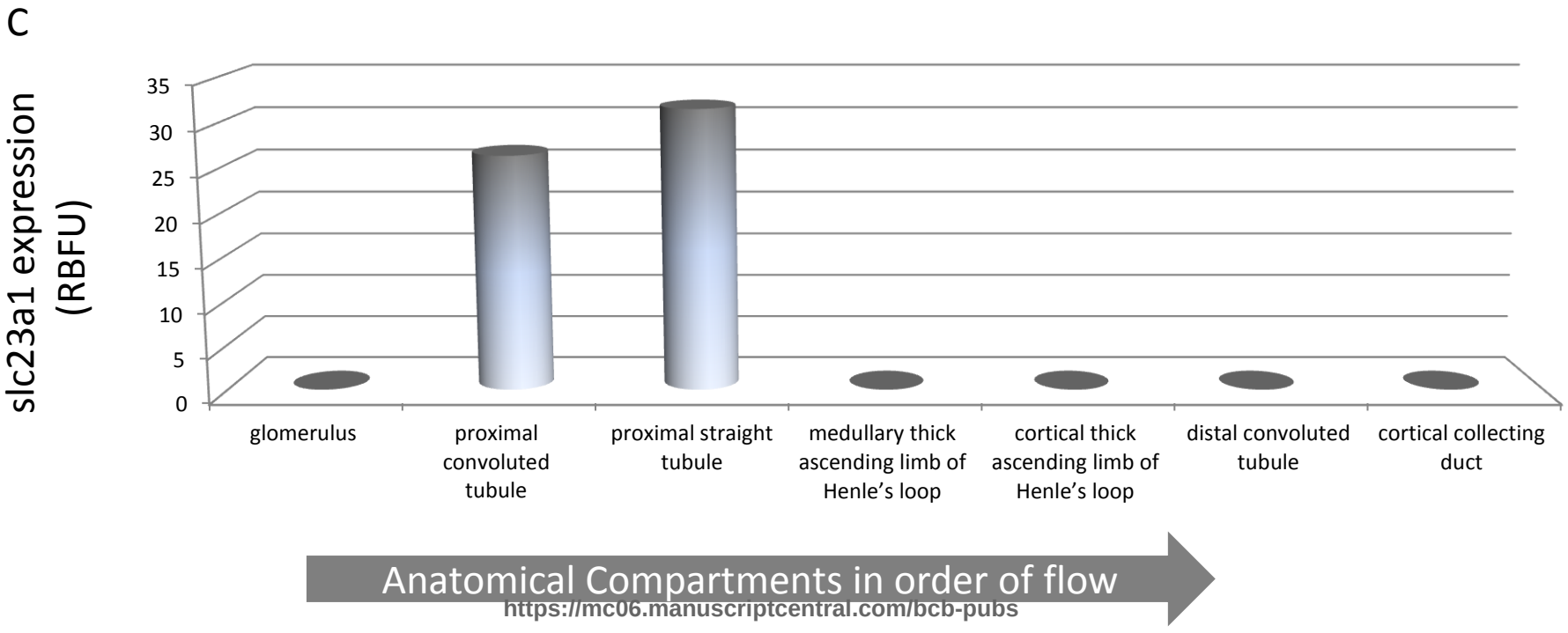
C
slc23a1 expression (RBFU)
35
30
25
20
15
10
5
0
glomerulus
proximal convoluted tubule
proximal straight tubule
medullary thick ascending limb of Henle's loop
cortical thick ascending limb of Henle's loop
distal convoluted tubule
cortical collecting duct
Anatomical Compartments in order of flow

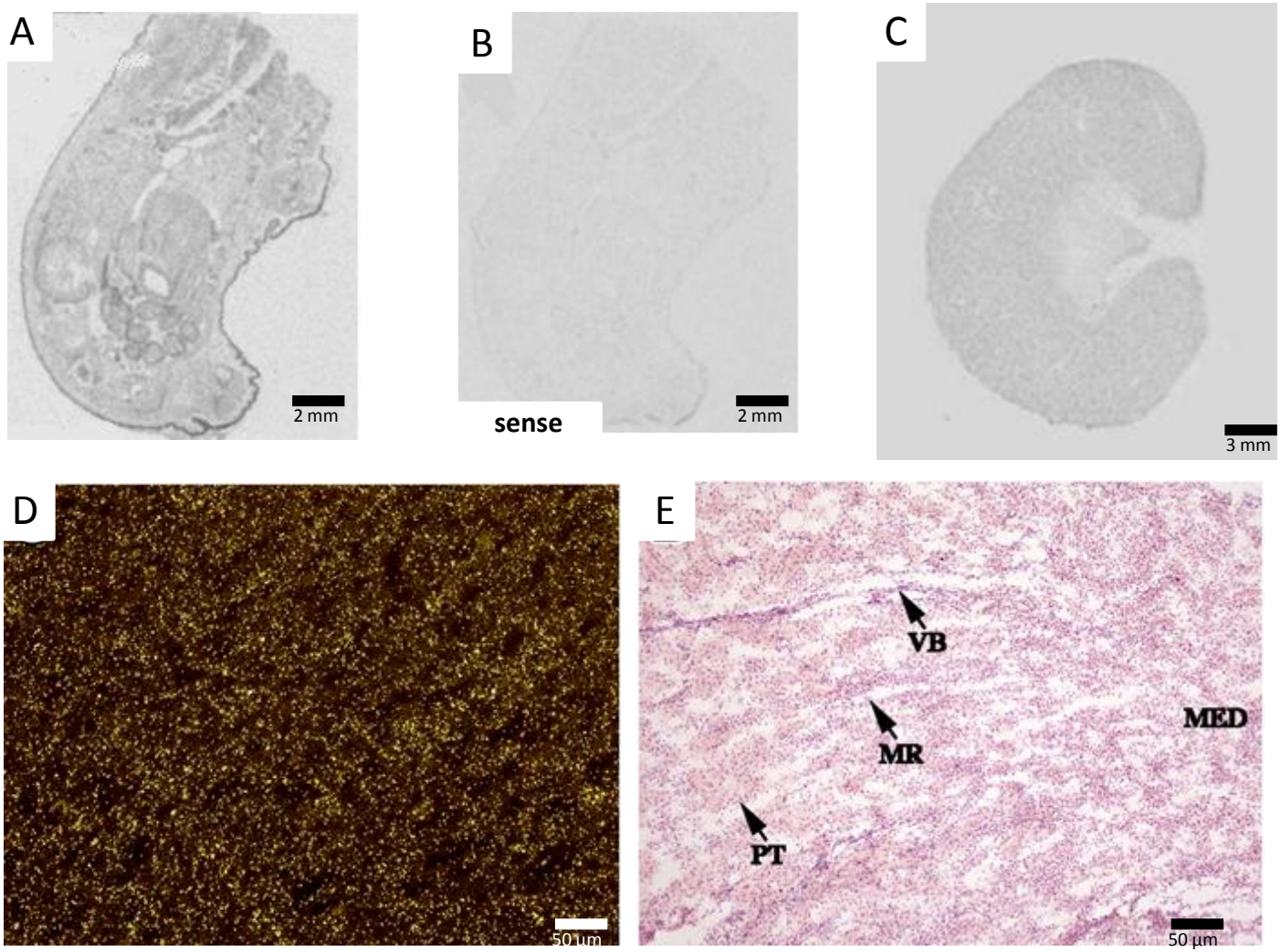
A
2 mm
B
sense
2 mm
C
3 mm
D
50 µm
E
VB
MR
PT
MED
50 µm

F

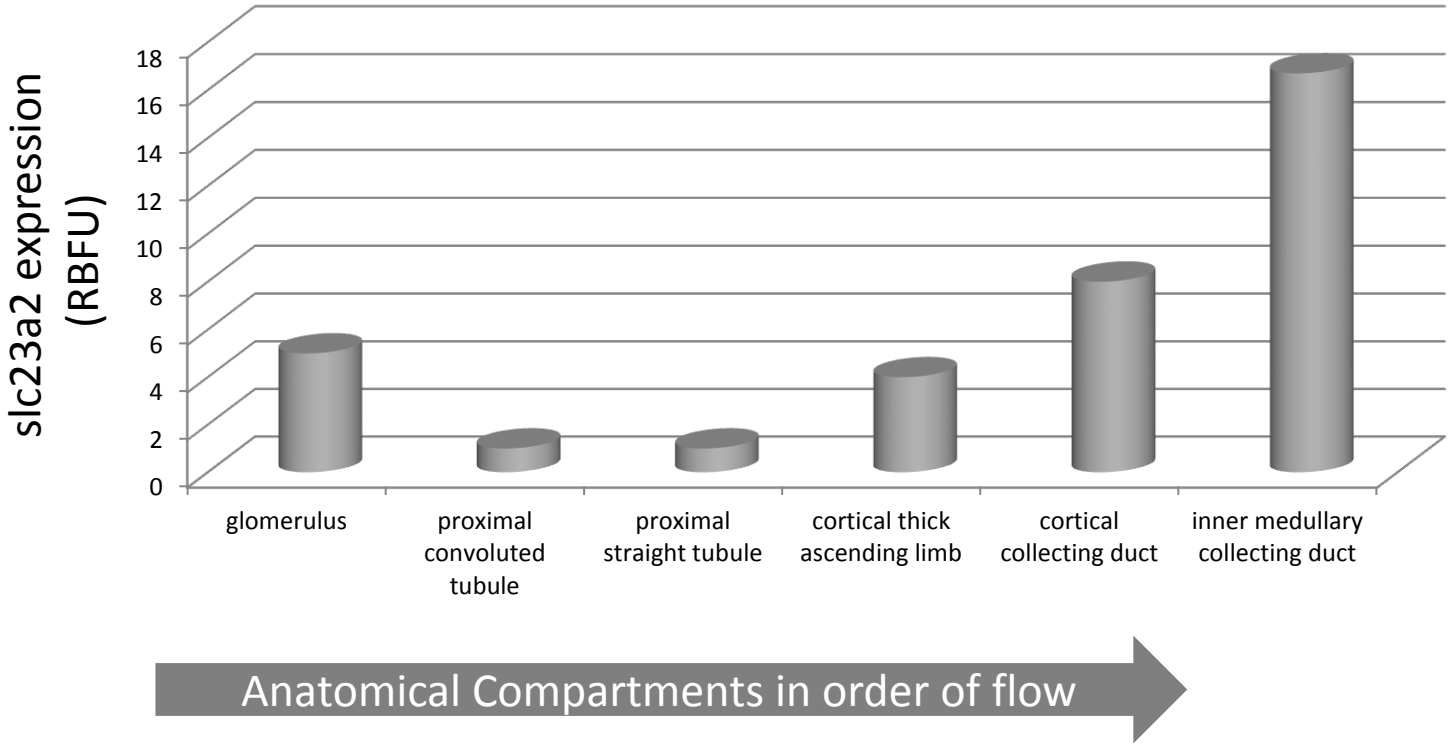
slc23a2 expression (RBFU)
0
2
4
6
8
10
12
14
16
18
glomerulus
proximal convoluted tubule
proximal straight tubule
cortical thick ascending limb
cortical collecting duct
inner medullary collecting duct
Anatomical Compartments in order of flow